



Contents lists available at ScienceDirect

Journal of Colloid and Interface Science

www.elsevier.com/locate/jcis



Regular Article

Synthesis and foaming properties of new anionic surfactants based on a renewable building block: Sodium dodecyl isosorbide sulfates

Aurélie Lavergne^a, Ying Zhu^a, Aldo Pizzino^b, Valérie Molinier^{a,*}, Jean-Marie Aubry^a^a Université Lille Nord de France, USTL, ENSCL, E.A. 4478 Chimie Moléculaire et Formulation, Cité Scientifique, 59652 Villeneuve d'Ascq Cedex, France^b Universidad de Los Andes, Laboratorio FIRP, Ingeniería Química, Mérida, Venezuela

ARTICLE INFO

Article history:

Received 2 March 2011

Accepted 28 April 2011

Available online xxxxx

Keywords:

Isosorbide

Sorbitol

Sodium dodecyl sulfate

Lauryl ether sulfate

Anionic surfactant

Critical micelle concentration

Krafft temperature

Foam stability

ABSTRACT

Two agro-based anionic surfactants containing an isosorbide moiety have been synthesized and their amphiphilic properties evaluated. Since isosorbide is now considered as an important platform chemical of the starch industry, these compounds could represent bio-sourced alternatives to the alkyl ether sulfates (notably lauryl ether sulfate, LES) that are based on petroleum-derived ethylene oxides. As isosorbide is an asymmetric diol, two isomers can be prepared (2-*O*-dodecyl isosorbide sulfate and 5-*O*-dodecyl isosorbide sulfate) that show significantly different aqueous properties as regards to their Krafft temperatures and critical micellar concentrations. 5-*O*-dodecyl isosorbide sulfate is the most soluble and the most efficient surfactant. It possesses a much lower critical micelle concentration (cmc) than sodium dodecyl sulfate, SDS, leading to comparable foaming properties with a three times lower concentration. Its behavior compares well with the one of pure diethoxylated dodecyl sulfate that has also been prepared and evaluated in this work.

© 2011 Elsevier Inc. All rights reserved.

0. Introduction

Anionic surfactants, including soaps, account for more than 60% of the total world production of surface active species, a market that altogether reached 12 mt/year in 2007 and is currently progressing at a rate of 3%/year [1]. The most important synthetic anionic surfactants in volume today are the alkylbenzenesulfonates (ABS), followed by the ethoxylated alkyl sulfates (AES) and alkyl sulfates (AS). They are found mainly in detergents, household and industrial cleaning products and also, for the latter two, in cosmetics and pharmaceuticals, especially in personal care formulations such as shampoos [2]. The formulation of such end-use products has to face severe environmental and toxicological issues. Notably, the environmental impact of detergents is strictly regulated as for instance by European directive 73/405/CE imposing a global biodegradability for detergents higher than 90% and for ionic surfactants higher than 80%. For all the three classes of anionic surfactants mentioned above, a biodegradability improvement has been obtained by replacing branched alkyl chains by linear ones in the lipophilic part of the surfactant. Regarding the anaerobic biodegradation, the linear alkyl benzene sulfonates (ABS) are regarded as “poorly biodegradable”, whereas the sulfated surfactants (AS and AES) are “well biodegradable” [2].

If we consider the endeavor today to look for products that fulfill the criteria of “sustainable development” [3], the search for renewable raw materials for the production of surfactants and other compounds for formulation is a research area of intensive interest. The demands on the molecular structure of these compounds become even stricter if one wants to get quality label of the final products. For instance, for an “EcoCert” label of cosmetics or detergents, it is forbidden to use ingredients that have been obtained *via* some kinds of chemical reactions, among which the ethoxylation. These kinds of restrictions are particularly harsh for surface-active species, since polyethoxylated chains are ubiquitous in polar heads of surfactants. If we take the example of the two most common AS and AES, respectively sodium dodecyl sulfate (SDS) and sodium lauryl ether sulfate (SLES), the introduction of 2–3 ethylene oxide (EO) units between the dodecyl chain and the sulfate polar head allowed to increase performances and decrease skin irritation. More generally, it was shown that the introduction of a few ethylene oxide units in the molecular structure of alkyl sulfates increased the water solubility and improved the surface active properties by lowering the critical micelle concentration (cmc) values [2]. If we go a step further, the concept of “extended surfactants” is starting to be well-documented [4,5]. This term refers to anionic surfactants (generally sulfates) including in their molecular structure several units of propylene oxides (PO) and ethylene oxides (EO) between the lipophilic alkyl chain and the sulfate group. These kinds of surfactants have proven to exhibit unusual solubilizing properties towards triglycerides due to the gradual increase of polarity along the molecular chain. To follow

* Corresponding author.

E-mail address: valerie.molinier@univ-lille1.fr (V. Molinier).

the current trend to replace petroleum-derived products by alternatives derived from renewable alternatives, it would thus be of the utmost interest to find “green” hydrophilic synthons able to stand for the petroleum-derived ethylene oxides.

Isosorbide is a well-defined “sustainable” diol readily obtained from sorbitol by a double dehydration and it is an important product of the starch industry. Its substantial availability makes researchers find new applications for its use. Recently, several authors are evaluating its use as a hydrophilic synthon to design various derivatives, ranging from solvents to surfactants [6–8]. Isosorbide is however not hydrophilic enough to balance an alkyl chain longer than six carbons, and for the design of surfactants, it would rather act as a “hydrophilic linker” that can be inserted between the lipophilic alkyl chain and the polar head. From a structural point of view, isosorbide is a V-shaped molecule consisting of two fused tetrahydrofuran rings. The two hydroxyl groups in *endo*- and *exo*-orientations are sterically and electronically non-equivalent, and consequently two series of compounds are obtained depending on the position of substitution. In the present work, isosorbide has been inserted between a dodecyl alkyl chain and a sulfate group to obtain ionic surfactants comparable to SDS and sodium diethoxylated dodecyl sulfate (SLE₂S) (Fig. 1). The SLE₂S used here is not a commercial blend but has been prepared from diethylene glycol and thus contains exactly 2 ethylene oxide (EO) units. Due to its rigid structure, the isosorbide synthon is expected to modify significantly the aggregation and surface properties, which has been evaluated by measuring the critical micelle concentration (cmc), Krafft temperature and foaming properties of the compounds.

1. Experimental

1.1. Chemicals and general methods

1-bromododecane (Alfa Aesar, 98%), anhydrous lithium hydroxide (Alfa Aesar, 98%), dimethylsulfoxide (DMSO) (Acros, 99.7%), diethylene glycol (Aldrich, 98%), sulfur trioxide pyridine complex (Aldrich, 98%), N,N-dimethylformamide (DMF) (Aldrich, 99.8%) and metallic sodium (Prolabo) were used for the syntheses. The solvents for extractions and column chromatography were from SDS-Carlo Erba (synthesis grade). Isosorbide was a gift from Roquette (Lestrem) (>99%).

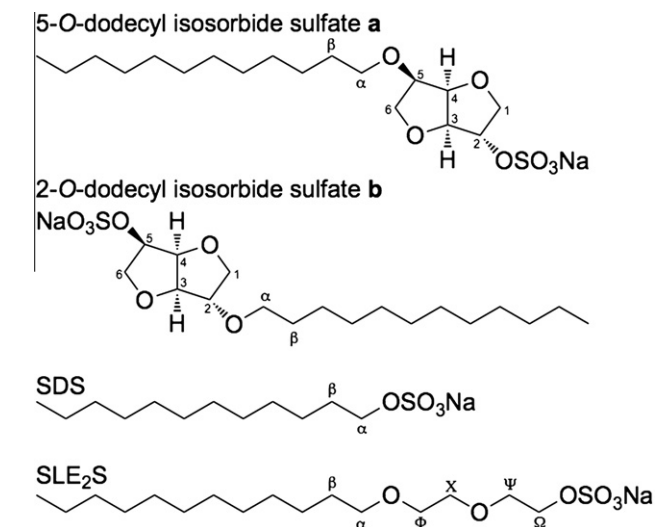


Fig. 1. The sodium dodecylisosorbide sulfate surfactants under study (**a** and **b**) in comparison with sodium dodecyl sulfate (SDS) and sodium diethoxylated dodecyl sulfate (SLE₂S).

SDS was obtained from Merck-Prolabo (98%).

For all experiments, ultra-pure water (resistivity 18.2 MΩ cm) was used.

Thin layer chromatography (TLC) was performed on silica gel plates and visualized by spraying a 10% v/v ethanolic solution of sulfuric acid followed by heating of the plate. SDS silica 60A C.C. (35–70 μm) was used for chromatography.

NMR spectra were recorded on Bruker AC spectrometers at 300.13 MHz for ¹H and 75.47 MHz for ¹³C.

High resolution mass spectra were performed by the “Centre Universitaire de Mesures et d’Analyses de l’Université de Lille 2”, on an Exactive (Thermo Fisher Scientific).

1.2. Synthesis and purification of the compounds

1.2.1. Sodium dodecylisosorbide sulfates **a** and **b**

The compounds studied were obtained by sulfation of 2-*O*- and 5-*O*-monododecyl isosorbide with Pyr.SO₃ complex. 2-*O*- and 5-*O*-monododecyl isosorbide were obtained by direct alkylation of isosorbide by bromododecane as described in references [8,9]. The sulfation route is described below for compound **a**, and is identical for compound **b**.

5-*O*-monododecyl isosorbide (11.6 g, 37 mmol) is dissolved in DMF (15 mL) at room temperature and Pyr.SO₃ complex (6.46 g, 41 mmol, 1.1 eq) is added. The reaction medium is left under stirring at room temperature for one hour. After this period of time, only traces of unreacted 5-*O*-monododecyl isosorbide are observed on TLC. DMF is then evaporated under reduced pressure to give a yellowish waxy crude residue. This residue contains mainly the pyridinium salt of the 5-*O*-monododecyl isosorbide sulfate, which is obtained in the pure form after flash chromatography with elution of dichloromethane/methanol 100/0 v/v to 90/10 v/v (14.25 g, 30 mmol, 81%). To exchange the pyridinium counterion with sodium, the compound is introduced in a 30 mL methanolic solution in which 695 mg (30 mmol, 1 eq) of metallic sodium have previously been introduced. The sodium salt precipitates and the medium is left under stirring at room temperature for 30 min to ensure completion. The suspension is then centrifugated and the supernatant is removed. In order to remove all traces of pyridine from the compound, methanol is added again to the powder. The suspension is sonicated for a few minutes, centrifugated and the supernatant is removed. This operation is repeated three times and the final powder is dried overnight at 40 °C under vacuum (3 × 10⁻² mbars). Final purification is carried out by performing two consecutive recrystallisations from 1-propanol. The pure sodium salt of the 5-*O*-monododecyl isosorbide sulfate **a** is obtained as a white powder.

The purity of the compounds was ascertained by ¹H and ¹³C NMR spectroscopy. The NMR spectra of the two compounds are given below. For the numbering of the carbons on the isosorbide cycle, see Fig. 1.

5-*O*-dodecyl isosorbide sulfate a. ¹H NMR (300 MHz, D₂O): δ 0.77 (3H, t, *J*_{CH₂-CH₃} = 6.5 Hz, CH₃), 1.08–1.30 (18H, m, 9 CH₂), 1.40–1.60 (2H, m, CH_{2β}), 3.35 (1H, td, *J*_{Hα1-Hα2} = 9.1 Hz, *J*_{Hα-Hβ} = 6.9 Hz, CH_{2α1}), 3.44 (1H, dd, *J*_{H6a-H6b} = 8.2 Hz, *J*_{H6-H5} = 8.2 Hz, H_{6a}), 3.58 (1H, td, *J*_{Hα1-Hα2} = 9.1 Hz, *J*_{Hα-Hβ} = 6.9 Hz, CH_{2α2}), 3.81–3.92 (2H, m, H_{1a}, H_{6b}), 3.94–4.08 (2H, m, H_{1b}, H₅), 4.60–4.69 (2H, m, H₃, H₄), 4.73 (1H, d, *J*_{H2-H3} = 3.3 Hz, H₂). ¹³C NMR (75 MHz, D₂O): δ 13.80 (CH₃), 22.64–25.99–29.54–29.57–29.67–29.88–29.91–29.94–29.97–32.00 (10 CH₂), 69.85 (C₆), 70.71 (CH_{2α}), 73.19 (C₁), 79.64 (C₅), 80.12 (C₄), 82.05 (C₂), 85.95 (C₃). HRMS: [M+H]⁺ C₁₈H₃₄O₇NaS, calculated: 417.1917, found: 417.1915.

2-*O*-dodecyl isosorbide sulfate b. ¹H NMR (300 MHz, DMSO): δ 0.86 (3H, t, *J*_{CH₂-CH₃} = 6.6 Hz, CH₃), 1.18–1.32 (18H, m, 9 CH₂), 1.39–1.52 (2H, m, CH_{2β}), 3.35–3.48 (3H, m, CH_{2α}, H_{6a}), 3.70–3.86 (4H, m, H_{6b}, H_{1a/b}, H₂), 4.35–4.40 (1H, m, H₃), 4.43 (1H, dd,

$J_{H4-H3} = J_{H4-H5} = 4.5$ Hz, H_4), 4.46–4.54 (1H, m, H_5). ^{13}C NMR (75 MHz, DMSO): δ 14.43 (CH_3), 22.56–26.05–29.18–29.29–29.46–29.49–29.62–29.69–29.73–31.76 (10 CH_2), 69.10 (C6), 69.37 ($\text{CH}_{2\alpha}$), 72.96 (C1), 75.76 (C5), 80.80 (C4), 84.24 (C2), 84.98 (C3). HRMS: $[\text{M}+\text{H}]^+$ $\text{C}_{18}\text{H}_{34}\text{O}_7\text{NaS}$, calculated: 417.1917, found: 417.1918.

1.2.2. Sodium diethoxylated dodecyl sulfate (SLE₂S)

SLE₂S was synthesized by sulfation of diethoxylated dodecyl alcohol as described above for compounds **a** and **b**. Diethoxylated dodecyl alcohol (C_{12}E_2) was obtained by reaction of dodecyl bromide with diethyleneglycol in Williamson conditions as described in references [10,11] for C_{10}E_4 .

SLE₂S was recrystallized twice from 1-propanol and its purity was ascertained by ^1H and ^{13}C NMR spectroscopy. For the numbering of the carbons, see Fig. 1.

Sodium diethoxylated dodecyl sulfate SLE₂S. ^1H NMR (300 MHz, D_2O): δ 0.83 (3H, t, $J_{\text{CH}_2-\text{CH}_3} = 6.4$ Hz, CH_3), 1.17–1.33 (18H, m, 9 CH_2), 1.48–1.60 (2H, m, $\text{CH}_{2\beta}$), 3.43 (2H, t, $J_{\text{CH}_2\beta-\text{CH}_2\alpha} = 6.6$ Hz, $\text{CH}_{2\alpha}$), 3.53–3.59 (2H, m, $\text{CH}_{2\phi}$), 3.60–3.67 (2H, m, $\text{CH}_{2\chi}$), 3.69–3.75 (2H, m, $\text{CH}_{2\psi}$), 4.08–4.15 (2H, m, $\text{CH}_{2\omega}$). ^{13}C NMR (75 MHz, D_2O): δ 13.80 (CH_3), 22.61–25.92–29.14–29.50–29.57–29.83–29.84–29.87–29.91–31.96 (10 CH_2), 67.43 ($\text{CH}_{2\omega}$), 68.98 ($\text{CH}_{2\psi}$), 69.35 ($\text{CH}_{2\phi}$), 69.68 ($\text{CH}_{2\chi}$), 71.09 ($\text{CH}_{2\alpha}$). HRMS: $[\text{M}+\text{H}]^+$ $\text{C}_{16}\text{H}_{34}\text{O}_6\text{NaS}$, calculated: 377.1968, found: 377.1967.

1.2.3. Sodium dodecyl sulfate (SDS)

Commercial SDS was recrystallized twice from ethanol.

1.3. Conductimetry measurements

Conductivity measurements were performed with a CDM 210 Conductimeter equipped with conductivity cell of cell constant = 0.865 cm^{-1} (Radiometer analytical).

1.3.1. cmc

cmc were determined by measuring the conductivity of aqueous solutions of the compounds of increasing concentrations. The solutions were thermostated at 25.0 °C or 45.0 °C and maintained under agitation with a magnetic stirrer during the measurements. The cmc is given by the slope break in the conductivity vs. concentration curve.

1.3.2. Krafft temperature

Clear 1% wt-solutions of surfactant were prepared and left to cool at -20 °C in the freezer overnight to ensure complete precipitation of the compounds in the form of hydrated crystals. The conductivity of the solution was then measured under stirring at a temperature controlled at ± 0.1 °C with a thermostated bath. The temperature was tuned 0.5 °C by 0.5 °C from 10.0 °C to at least 5 °C above the Krafft temperature. The solution was left to equilibrate 5 min at the desired temperature before reading the conductivity value. The Krafft temperature is given by the slope break in the conductivity vs. temperature curve. This temperature is the same as that required to completely dissolve the hydrated solid surfactant, judged visually to be the point of complete clarification of the solution.

1.4. Molecular modeling

The two isosorbide surfactants have been drawn using ArgusLab 4.0.10 [12] and optimized with ArgusLab UFF. Next, DFT calculations were performed using Turbomole 5.1 [13] and the DFT functional B88-PW86 with a triple zeta valence polarized basis set (TZVP). The continuum solvation model COSMO [14] has been

applied in order to simulate a virtual conductor environment for the molecule, generating a more polarized electron density than in vacuum.

1.5. Foaming properties

1.5.1. Modified Bikerman's test

The foaming properties of aqueous solutions of the compounds were determined using a modified Bikerman's test. 10 mL of solutions were introduced in a double-jacked column of 3.5 cm internal diameter. The column was thermostated at 25.0 °C. Pre-humidified N_2 was introduced in the solution via a 0.8 mm diameter syringe at a 45 mL/min flow rate. The foam formation was followed over time and the N_2 flow rate was stopped once the foam had attained its dynamic equilibrium [15], i.e. once the height remained constant. The foam stability was then assessed by plotting the evolution of the foam height with time.

1.5.2. High-speed shearing and measurements of light transmission and backscattering (Turbiscan[®]) [16]

The foaming properties of aqueous solutions of the compounds were also determined using the Turbiscan[®] Lab-Expert (Formulation, France). 10 mL of the solution was placed in a 25 mL flask and sheared with an Ultra-Turrax (IKA T10) during 5 min at 11,400 rpm to create foam. The sample was then immediately introduced in the Turbiscan[®] apparatus and transmitted and backscattered lights were measured along the sample height each minute during 1 h and then each ten minutes during 10 h.

For the two tests, foamability was evaluated by the foam height generated after a given period of time (20 min for the Bikerman's test, just after 5-min shearing for the other test). The foam stability was given by the half-life time $t_{1/2}$ defined as the time needed to get a reduction of half the initial height of the foam. For each experiment, the data were averaged over two measurements and reproducibility was found to be good.

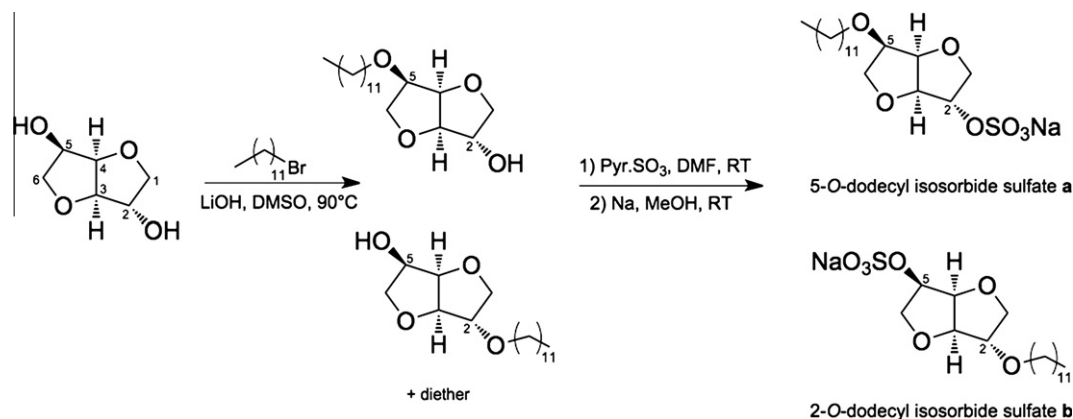
2. Results and discussion

2.1. Synthesis of the 5-O-dodecyl isosorbide sulfate **a** and 2-O-dodecyl isosorbide sulfate **b**

The monododecyl ethers of isosorbide were synthesized by direct alkylation of isosorbide by bromododecane, in the presence of lithium hydroxide in dimethylsulfoxide [8,9]. These reaction conditions promote selectivity towards the 5-O-alkyl isomer due to the higher acidity of proton OH-5 that establishes a hydrogen bond with the oxygen atom of the adjacent cycle (Scheme 1). Typical yields in monoethers are close to 40%, with selectivity towards 5-O-dodecyl isosorbide of ca. 87%.

The chosen route for sulfation is the one used by Linhardt and co. for the synthesis of sulfosucrose derivatives [17,18]. This mild reaction route was chosen instead of the usual reaction with chlorosulfonic acid to avoid any possible degradation of the isosorbide moiety leading to undesired side-products. The O-sulfo group is introduced by treating an OH-containing compound with a complex of sulfur trioxide (SO_3) and a Lewis base (in our case pyridine). In the case of polyols, sulfonation of the primary hydroxyl groups occurs first and the secondary ones are sulfonated afterwards. In our case, whatever the dodecylisosorbide isomer, the reaction proceeds nearly to completion very quickly, the yield of isolated products being over 80%.

It is important to note here that the synthetic path described above is clearly not applicable at an industrial scale, first because of the expensive sulfating agent used and then as regards to the purification technique chosen, as column chromatography is hardly



Scheme 1. Synthetic path to the sulfated dodecylisosorbide derivatives **a** and **b**.

Table 1
Krafft temperatures (1% w/w), critical micelle concentrations (cmc) and ionization degrees obtained by conductimetry for the isosorbide derivatives **a** and **b**, SDS and SLE₂S. In italics between brackets, the literature values from ref [21].

Compound	<i>T</i> Krafft (°C)	cmc at 25 °C (mmol L ⁻¹)	Ionization degrees at 25 °C	cmc at 45 °C (mmol L ⁻¹)	Ionization degrees at 45 °C
5-O-dodecyl isosorbide sulfate a	15	2.3	0.53	2.2	0.51
2-O-dodecyl isosorbide sulfate b	42	–	–	6.7	0.59
SDS	15	9.0 (7.94)	0.38	9.4	0.41
SLE ₂ S	<0	3.1 (2.88)	0.65	3.3 (2.78)	0.66

feasible at large-scale. The synthetic path is not either compliant with “sustainable development”, because of the reactants used, in the alkylation step for example. The aim here was to get the desired compounds in substantial amounts for physico-chemical characterization. If the compounds appear to have interesting properties, the investigation of an alternative synthesis will be considered.

2.2. Krafft temperature and cmc of dodecyl isosorbide sulfates compared to SDS and SLE₂S

The solubility of ionic surfactants in water is highly temperature-dependent. The solubility is very low at low temperature and increases dramatically with temperature in a very narrow temperature range [2]. The onset of solubility increase is named “Krafft Temperature” and this value is a characteristic of the studied surfactant particularly important for water applications. Under this temperature, the surfactant is in the solid crystalline state. At

the Krafft Temperature, the solubility of the surfactant in water is high enough to allow the formation of micelles, and therefore corresponds to the onset of the surfactive efficiency of the compound. In practice, the lower the Krafft Temperature, the more efficient the surfactant is in hot and cold water applications.

Table 1 gives the values of the Krafft temperatures measured for both dodecyl isosorbide sulfates, SDS and SLE₂S. These values are obtained at the slope-break of the Conductimetry vs. Temperature curves for 1% w/w solutions. The value obtained in this work for SDS is in good agreement with previous works carried out with the same method [19,20].

It is well known that the Krafft Temperature is strongly dependent on the alkyl chain length, the type of polar head, particularly the nature of the counter-ion, and headgroup interactions (including hydrogen bonding). In our case, all surfactants possess the same alkyl chain, polar head and counter-ion, therefore the variations in Krafft Temperatures can be discussed in terms of modifications of

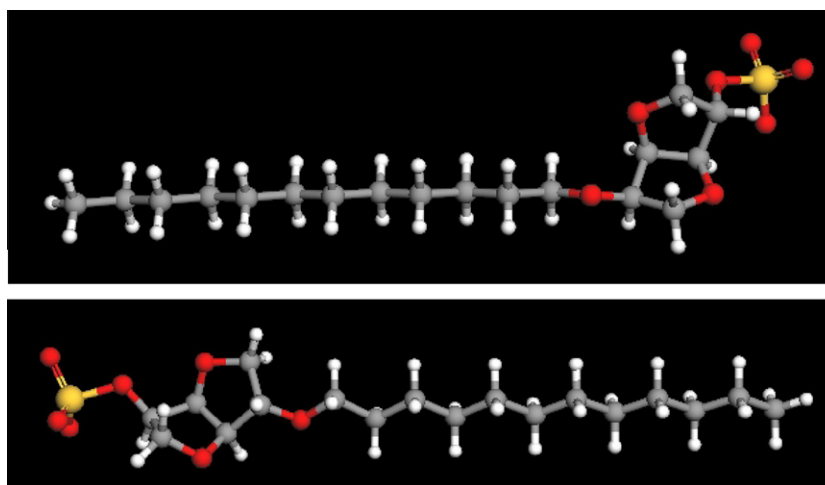


Fig. 2. Spatial conformation of 5-O-dodecyl isosorbide sulfate **a** (top) and 2-O-dodecyl isosorbide sulfate **b** (bottom) after geometry optimization (B3LYP/TZVP).

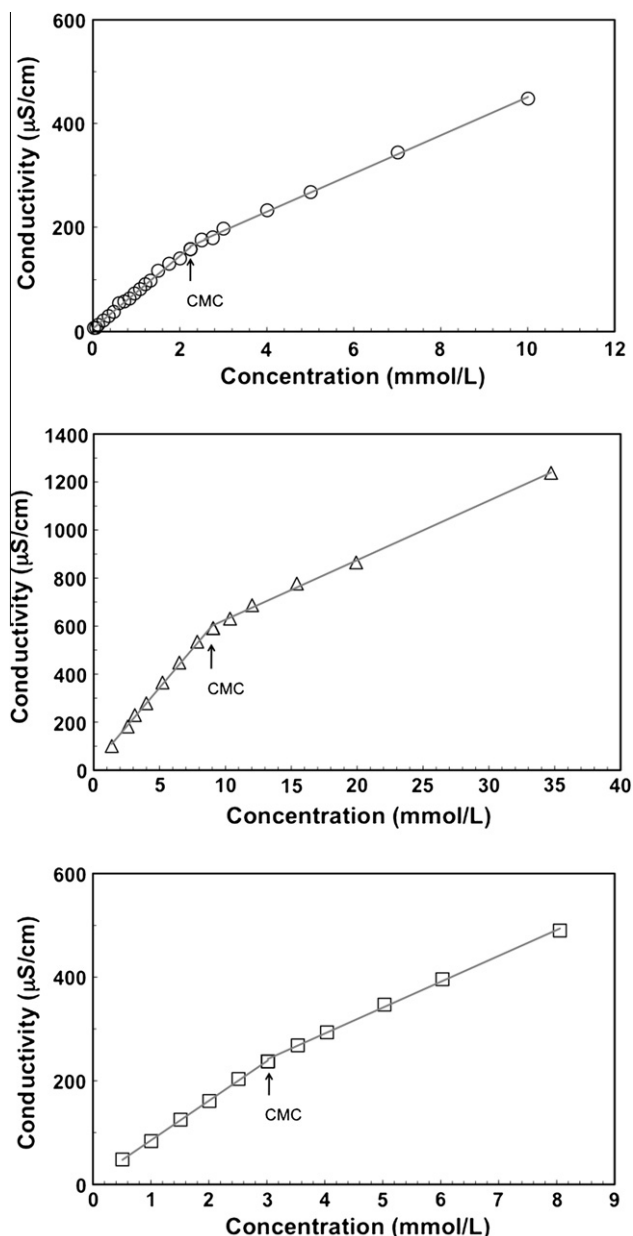


Fig. 3. Conductivity as a function of concentration for 5-O-dodecyl isoribide sulfate **a** (circle), SDS (triangle) and SLE₂S (square) at 25.0 °C.

the surfactant conformation linked to the type of hydrophilic linker between the hydrophobic chain and the polar head: none in the case of SDS, an isoribide moiety in two different configurations for compounds **a** and **b**, and a diethylene oxide group in the case of SLE₂S.

When a polar segment is introduced between the alkyl chain and the ionic group of an ionic surfactant, the Krafft temperature is usually reduced [2], as it is observed in the case of SLE₂S, the Krafft temperature of which falling below zero. In the case of isoribide however, two cases are found. For 5-O-dodecyl isoribide sulfate **a**, no reduction is observed compared to SDS whereas a large increase is observed for 2-O-dodecyl isoribide sulfate **b** which has a Krafft temperature 27 °C higher than the one of SDS. This high Krafft Temperature makes compound **b** unsuitable for water applications under 42 °C.

These observations show the limited hydrophilicity brought by the isoribide synthon and the large impact of isomeric effects on the properties in aqueous solutions. Indeed, the Krafft temperature

depends on the energy relationships between the solid crystalline state and the micellar solutions. In the case of short-chain monoalkyl ethers of isoribide, a noticeable difference in polarity had been observed between 5-O and 2-O isomers [8,11] that was linked to the preservation of an intramolecular hydrogen bond in the latter case. The marked difference in the Krafft temperature of the surfactants under study in the present work cannot be attributed to the same electronic effect, since both hydroxyl groups of isoribide are substituted. In this case, conformational effects linked to the rigidity imposed by the V-shaped isoribide moiety should be taken into account and one way to evaluate these effects is through molecular modeling. The optimized geometries evidence that 5-O-dodecyl isoribide sulfate **a** adopts a significantly more folded conformation compared to 2-O-dodecyl isoribide sulfate **b** (Fig. 2). For 5-O-dodecyl isoribide sulfate **a**, hydrophilicity brought by isoribide is strictly compensated by a poor trend to crystallize, resulting in the same Krafft temperature as SDS. The more linear conformation of **b** seems to result in a more efficient packing in the solid state, inducing a strong trend to crystallize that is, in this case, not compensated by the increase of hydrophilicity, and thus inducing a higher Krafft temperature.

The cmc have been assessed by conductivity measurements. The evolution of the conductivity of solutions of increasing concentrations have been measured at 25 °C, close to room temperature for SDS, SLE₂S and 5-O-dodecyl isoribide sulfate **a**, and at 45 °C, above Krafft temperature of 2-O-dodecyl isoribide sulfate **b**, for the 4 surfactants. The data at 25 °C are presented in Fig. 3. In all cases, the plots present two linear parts with different slopes and the cmc is found at their intersection. The cmc values obtained from these data are presented in Table 1. For SDS and SLE₂S, the values at 25 °C, 9.0 mmol/L and 3.1 mmol/L respectively, are slightly higher than the ones given in literature that were obtained by surface tension measurements (7.94 mmol/L and 2.88 mmol/L respectively [21]).

For all surfactants under study, as expected for ionics [2], the temperature dependence of the cmc is very low (Table 1). Whatever the temperature, 5-O-dodecyl isoribide sulfate **a** exhibits the lowest cmc and is therefore the most efficient surfactant. At 45 °C, it is interesting to notice again the isomeric effect on the isoribide derivatives since 2-O-dodecyl isoribide sulfate **b** has a higher cmc than its isomer and also than SLE₂S. It is thus less efficient than these two surfactants but remains more efficient than SDS at this temperature.

The evolution of the conductivity with the surfactant concentration also allows estimating the degree of micelle ionization α by calculating the ratio between the slopes of the straight lines above and below the cmc [22–24]. Slope of the straight line above the cmc is smaller than the one below the cmc due to the formation of charged micelles. Consequently, some counterions are confined in the micelle and the degree of micelle ionization corresponds to the ratio between the average number of micelle-dissociated counterions and the total number of counterions. At 25 °C, the degrees of micelle ionization determined by this method are found equal to 0.38, 0.53 and 0.65 for SDS, 5-O-dodecyl isoribide sulfate **a** and SLE₂S respectively. The value obtained for SDS is slightly higher than in literature, Bales [25] gives a value of 0.27 at 25 °C for SDS. However, the trend found in the present work seems to indicate a higher ionization of the micelle, thus a weaker binding of the sodium counterion, when a linker is placed between the aliphatic chain and the sulfate group. The effect is however less pronounced in the case of isoribide than for diethyleneglycol. The α values determined at 45 °C are indeed 0.41, 0.51, 0.59 and 0.66 for SDS, 5-O-dodecyl isoribide sulfate **a**, 2-O-dodecyl isoribide sulfate **b** and SLE₂S respectively. Insertion of a hydrophilic part seems to improve hydration of the surfactant headgroup and also to facilitate ionization [26]. It is also reported that the degree of

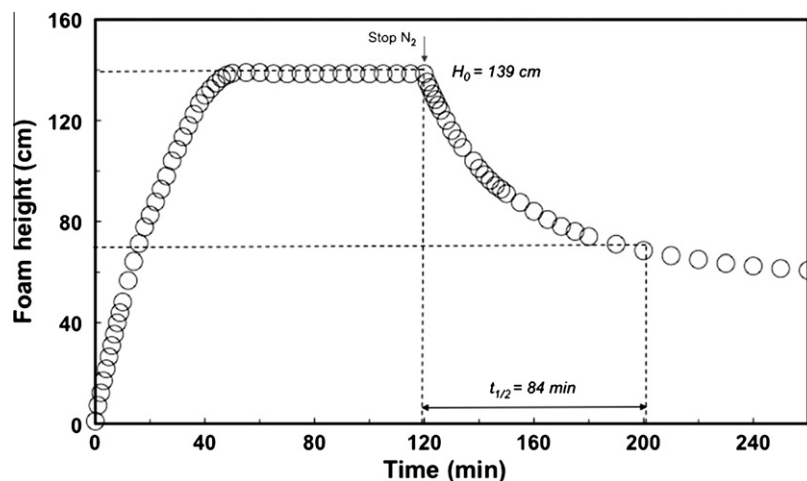


Fig. 4. Evolution of the foam height with time during a modified Bikerman's test for a solution of 5-O-dodecyl isoribide sulfate **a** ($C = 3 \text{ cmc} = 6.9 \text{ mmol/L}$, 2.9 g/L).

ionization depends on the micelle size: a large micelle has a higher tendency to attract counterions than a smaller one. SDS could form larger micelles than the three others surfactants. The effect of temperature on α is minor and we observe the same trend as at 25°C .

2.3. Foaming properties of 5-O-dodecyl isoribide sulfate **a** compared to SDS and SLE₂S

Due to a high Krafft temperature that is not compliant with applications in water at room temperature, the surface-active properties of 2-O-dodecyl isoribide sulfate **b** were not evaluated in this work. The following data only concern the 5-O-isomer **a**.

The evolution of the surface tension with concentration has been determined for all compounds and will be given and commented in a companion paper. Equilibrium surface tensions for solutions at 3 CMC equal 36.3, 39.6 and 41.2 mN/m respectively for SDS, SLE₂S and 5-O-dodecyl isoribide sulfate **a**. The insertion of a diethyleneglycol or an isoribide moiety between the alkyl chain and the sulfate group thus seems to reduce the surfactant efficiency, probably due to a less efficient packing at the interface.

In the present work, the surface activity of 5-O-dodecyl isoribide sulfate **a** has been investigated from a more applicative point of view by evaluating its foaming properties in comparison with SDS and SLE₂S. As the foaming power of a solution partly depends on the way the foam is generated, the aqueous foams

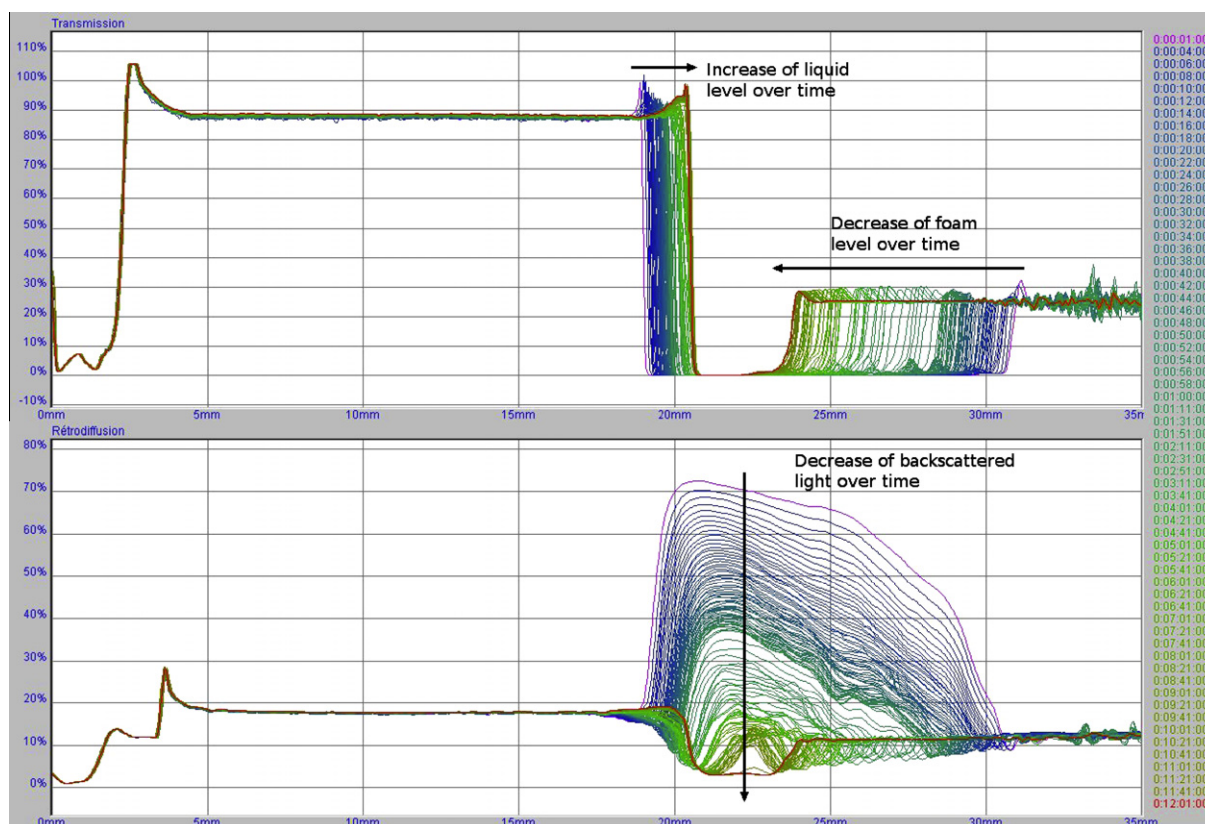


Fig. 5. Evolution of the transmitted (top) and backscattered (bottom) lights with time along the sample height (on the left hand side: bottom, on the right hand side: top of the glass vial) after generation of foam by high-speed shearing. Data obtained for a solution of 5-O-dodecyl isoribide sulfate **a** ($C = 3 \text{ cmc} = 6.9 \text{ mmol/L}$, 2.9 g/L).

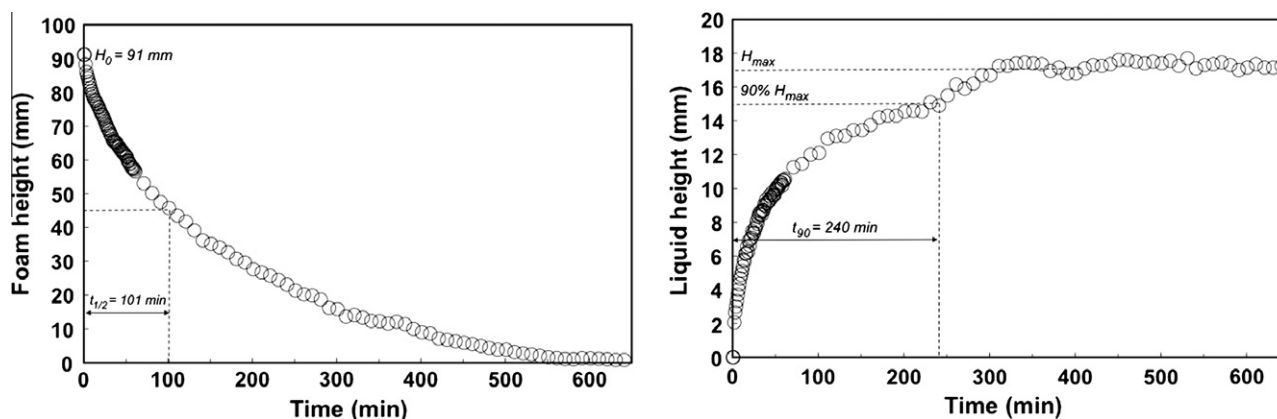


Fig. 6. Data that can be extracted from the transmitted light signal of the Turbiscan®: Evolution of foam height (left) and liquid height (drainage) (right) after generation of foam by high-speed shearing. The data shown were obtained for a solution of 5-*O*-dodecyl isosorbide sulfate **a** at a concentration equaling three times the cmc (6.9 mmol/L, 2.9 g/L).

Table 2

Quantitative data for the foams generated by solutions of 5-*O*-dodecyl isosorbide sulfate **a**, SDS and SLE₂S at a concentration equaling 3 times their respective cmcs, extracted from the two types of experiments. H_0 is the maximum foam height (Bikerman's) or height of foam formed after 5 min of shearing (high speed shearing). The time after which half of the initial foam height is lost is noted $t_{1/2}$ in both cases. For Bikerman's test, the height of foam formed during the first 20 first minutes is also given. For the high-speed shearing method, the initial percentage of water in foam is indicated and also the time to reach 90% of the final liquid level t_{90} (drainage).

Compound	C (mmol/L)	C (g/L)	Bikerman's test			High speed shearing			
			H_0 (cm)	$H_{20 \text{ min}}$ (cm)	$t_{1/2}$ (min)	H_0 (mm)	Water ($t = 0$)	$t_{1/2}$ (min)	t_{90} (min)
a	6.9	2.9	139	82	84	91	19%	101	240
SDS	27	7.8	130	67	147	114	16%	83	260
SLE ₂ S	9.3	3.5	138	60	186	63	17%	64	111

were obtained in two different manners, either by continuous injection of gas (modified Bikerman's test) or by high-speed shearing of the solutions. Both methods allow obtaining foamability defined here as the foam formed during a fixed period of time. The foam stability is evaluated by the half-life time $t_{1/2}$ defined as the time needed to get a reduction of half the initial height of the foam.

2.3.1. Foamability and foam stability at three cmc

A typical curve recorded during a modified Bikerman's test is presented in Fig. 4. It was obtained with a solution of 5-*O*-dodecyl isosorbide sulfate **a** at a concentration of 6.9 mmol/L corresponding to 3 times the value of its cmc. In all cases, the curves show three regimes: the foam generation while bubbling nitrogen, the attainment of a dynamic equilibrium when the foam formed at the bottom of the column is exactly balanced by the foam breaking at the top and finally the foam destruction after stopping gas injection.

For the high-speed shearing method, the foam formation cannot be followed, only the initial height of foam generated after a given shearing time is measured. The Turbiscan® apparatus allows recording the evolution of the transmitted and backscattered lights with time along the sample height (Fig. 5).

The light transmission equals ca. 90% in the liquid phase, 0% in the foam and about 25% in the air (due to diffusion on the walls of the vial). On the transmitted light signal, the location of the foam and liquid levels are clear. The evolution of foam height with time gives access to $t_{1/2}$ and the evolution of the liquid height with time shows out the foam drainage, which can be quantified by the time needed to reach 90% of the final liquid level t_{90} (Fig. 6). As both liquid and foam levels are determined at any time, the foam wetness can also be obtained knowing the geometric characteristics of the vial. The evolution of the backscattered light with time at a given location in the sample gives information on coalescence and Ostwald ripening destabilization phenomena since the back-

scattering intensity is conversely related to bubble size. The back-scattering intensity is maximum near the liquid/foam interface, indicating smaller air bubbles than at the top of the foam.

Data on foamability and foam stability are presented in Table 2 for the three surfactants at a concentration equaling 3 times their respective cmc.

2.3.1.1. Foamability. The maximum foam heights H_0 are relatively similar for the three surfactants when sparging gas is used to generate the foam (Bikerman). The initial slope of foam formation is however more important for 5-*O*-dodecyl isosorbide sulfate **a**, thus the foam height formed during the first 20 min is higher and H_0 is attained more rapidly for this surfactant than for the two others. On the contrary, the foam height formed after 5 min of high-speed

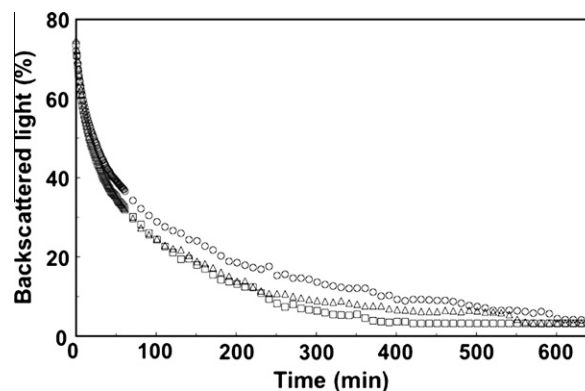


Fig. 7. Evolution with time of the backscattered light at the bottom of the foam for 5-*O*-dodecyl isosorbide sulfate **a** (circle), SDS (triangle) and SLE₂S (square). Foam generated by high-speed shearing.

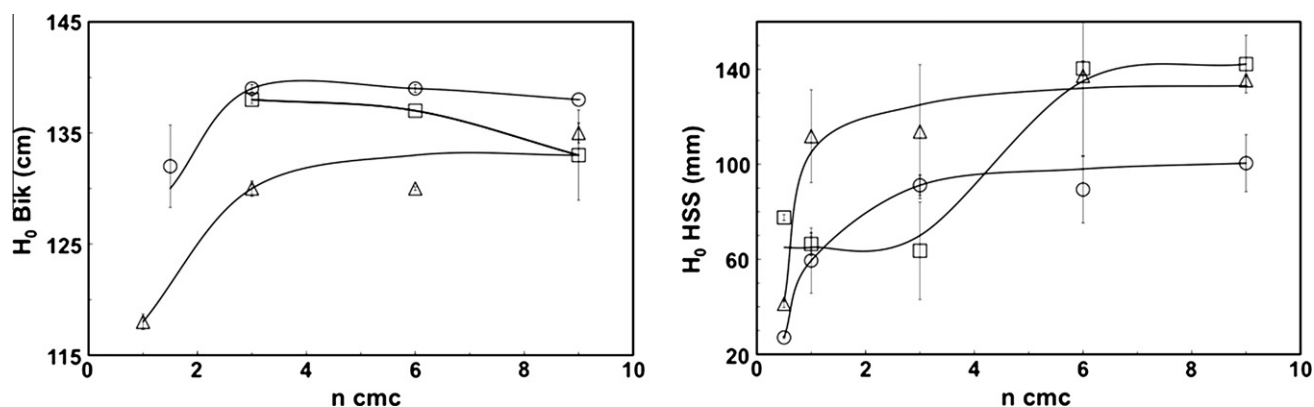


Fig. 8. Evolutions of initial foam height H_0 with surfactant concentration for 5-*O*-dodecyl isorbidide sulfate **a** (circle), SDS (triangle) and SLE2S (square). Foam generated by sparging gas (Bikerman's test, left) or high-speed shearing (right). The lines are drawn to guide the eye.

shearing is more important for SDS. It is well known that it is difficult to compare foam properties by different techniques, since they do not provide the same characteristics and do not generate the same types of foams [27]. In our case, the Bikerman's method produces quite dry foams with bubble diameter of about 5 mm (visual observation) compared to the high-speed shearing method that forms bubbles with a diameter between 100 and 200 μm (as evaluated from the backscattering light intensity [16]). Also, the Bikerman's test cannot separate foamability and foam stability, since while bubbling gas, the foam continuously forms at the bottom of the column and dies at the top, H_0 being taken when the equilibrium state is reached [15]. It can be said however that all surfactants possess comparable foamabilities at concentrations three times their respective cmcs, which is in favor of 5-*O*-dodecyl isorbidide sulfate **a** that owns the lower cmc (Tables 1 and 2).

2.3.1.2. Foam stability. The foam stability is evaluated by the half-life time $t_{1/2}$ given in Table 2 for the three surfactants at $C = 3$ cmc. Again, the method used has to be considered before drawing a comparison between the three surfactants. In the Bikerman's test, 5-*O*-dodecyl isorbidide sulfate **a** produces the least stable foam, with $t_{1/2}$ more than twice lower than the one of SLE₂S. As Bikerman's test does not provide any quantitative data to evaluate foam dryness nor to differentiate coalescence, Ostwald ripening and drainage, this difference in stability is difficult to discuss.

When foam is generated by high-speed shearing, the trend is inverted and 5-*O*-dodecyl isorbidide sulfate **a** appears to form the most stable foam. The initial backscattering intensity is similar

for the three samples, indicating similar bubble sizes (diameter close to 140 μm). However, an initial difference in foam wetness is observed as indicated in Table 2, the foam formed by 5-*O*-dodecyl isorbidide sulfate **a** having a higher water content. The evolution of liquid level with time for the three surfactants shows that drainage is twice quicker for SLE₂S (Table 2). The evolution of the backscattered light at the bottom of the foam is shown in Fig. 7 for the three surfactants. It decreases nearly at the same rate due to an increase of bubble size. This increase seems to be slightly slower for 5-*O*-dodecyl isorbidide sulfate **a**, which tends to indicate slightly reduced Ostwald ripening.

2.3.2. Effect of surfactant concentration on foaming properties

As the foaming properties of aqueous solutions of surfactants are known to depend on concentration, the two experiments, Bikerman's test and high-speed shearing method, have been performed at concentrations ranging from 0.5 cmc to 9 cmc for the three surfactants. The evolutions of H_0 and $t_{1/2}$ are plotted in Figs. 8 and 9.

During a Bikerman's experiment, the dynamic equilibrium cannot be reached for concentrations lower than cmc for SDS and 5-*O*-dodecyl isorbidide sulfate **a**. For SLE₂S, the equilibrium is not even reached at the cmc. The maximum foam height seems to increase with surfactant concentration until 3 cmc and does not depend strongly on concentration afterwards. The three surfactants possess similar foamabilities, with slightly better results for 5-*O*-dodecyl isorbidide sulfate **a**. When foams are formed by high-speed shearing, the same trends are observed, with a limit around

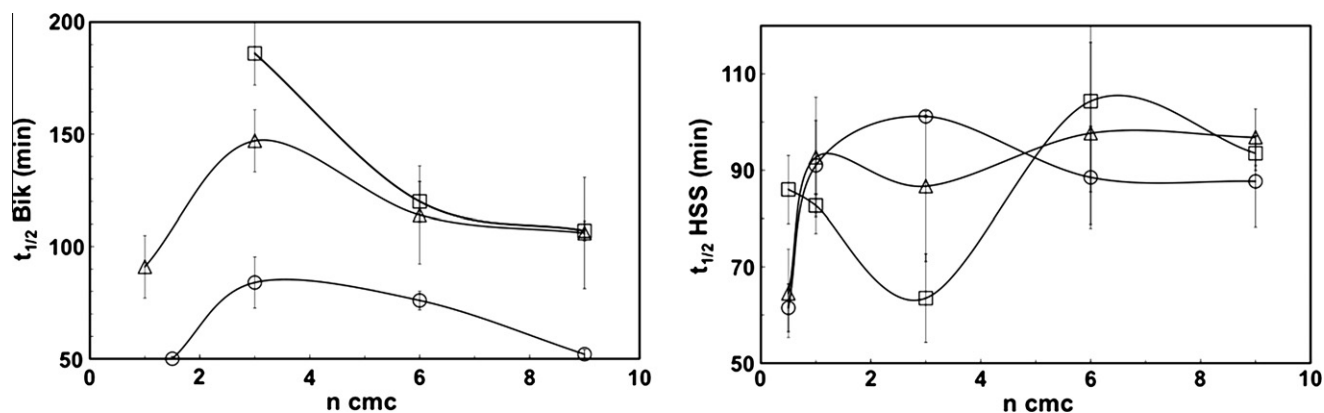


Fig. 9. Evolutions of half-life time $t_{1/2}$ with surfactant concentration for 5-*O*-dodecyl isorbidide sulfate **a** (circle), SDS (triangle) and SLE2S (square). Foam generated by sparging gas (Bikerman's test, left) or high-speed shearing (right). The lines are drawn to guide the eye.

3 cmc for 5-*O*-dodecyl isosorbide sulfate **a** and SDS and 6 cmc for SLE₂S. At intermediate concentration (3 cmc), 5-*O*-dodecyl isosorbide sulfate **a** has intermediate foamability, whereas at higher concentrations (6 cmc), its foamability is lower than the two other surfactants.

The foam stability seems to be more dependent on concentration for the Bikerman's experiment, for which $t_{1/2}$ decreases when the surfactant concentration increases once the maximum foamability is reached (for $C > 3$ cmc). Differences in foam stabilities are usually explained by differences in water drainage rate from the foam lamella. This drainage is itself influenced by the bulk viscosity, the fluidity of the film and Marangoni stabilization mechanisms [28]. In this test, 5-*O*-dodecyl isosorbide sulfate **a** forms the least stable foam whatever the concentration. When foam is generated by high-speed shearing, no real trend shows up and the three surfactants seem to behave similarly.

3. Conclusion

Two anionic surfactants have been synthesized from isosorbide, an asymmetric biosourced diol, by grafting a dodecyl alkyl chain on one hydroxyl group and sulfating the other one. Depending on the relative positions of the lipophilic and hydrophilic parts, two isomers are obtained with significantly different aqueous properties (Krafft temperature, critical micellar concentration), probably due to the fairly different conformations adopted and the rigidity of isosorbide.

5-*O*-dodecyl isosorbide sulfate **a** has the same Krafft temperature as SDS but its cmc is much lower, which makes it a more efficient surfactant. 2-*O*-dodecyl isosorbide sulfate **b** due to a more linear conformation packs more efficiently in the solid state and has a Krafft temperature higher than SDS.

The foaming properties have been evaluated by generating the aqueous foams in two different manners, either by sparging gas (Bikerman's test) or high-speed shearing the solution. The foaming properties of 5-*O*-dodecyl isosorbide sulfate **a** are comparable to the ones of SDS and SLE₂S, with slightly lower foam stability during Bikerman's test.

5-*O*-dodecyl isosorbide sulfate **a** is a good example of an efficient surfactant derived from an agro based synthon that could fulfill some of the criteria for eco-labellization of formulated products, provided that its biodegradability and human safety be proven and the synthetic path improved to allow the scaling up. These results are promising for the use of renewable building blocks in the preparation of surface active species, in place of the widespread petroleum-derived synthons. Here, isosorbide is shown to be a possible alternative to the polyethoxylates. This replacement requires investigating finely the effect of such structural changes on physico-chemical properties and self association in water of the surfactants. Renewable building blocks may bring not only a variation

in the hydrophilic/lipophilic balance but also a modification of conformation or flexibility of the molecule that impacts on the properties. In the case of pure alkyl glucosides, it has already been pointed out the different behaviors of α and β anomers, whereas the behavior of sucrose esters for instance is highly dependent of the acylation position.

Acknowledgments

CNRS is acknowledged for a grant to AL. The authors thank Région Nord Pas de Calais for financing the acquisition of the Turbiscan[®] apparatus through European FEDER funding.

The authors would also like to thank FONACIT (Venezuela) and the Ministère des Affaires Etrangères et Européennes (France) for financing the Postgraduate Cooperation Program PCP N° PCP 2010000308 "Green Emulsions".

References

- [1] M.I. Levinson, *Surfactant Sci. Ser.* 142 (2009) 1.
- [2] K. Holmberg (Ed.), *Handbook of Applied Surface and Colloid Chemistry*, vol. 1, John Wiley & Sons Ltd., 2002.
- [3] D.G. Hayes, D. Kitamoto, D.K.Y. Solaiman, R.D. Ashby (Eds.), *Biobased surfactants and detergents: synthesis, properties, and applications*, AOCS Press, 2009.
- [4] M. Minana-Perez, A. Graciaa, J. Lachaise, J.-L. Salager, *Colloids Surf., A* 100 (1995) 217.
- [5] L.D. Do, A. Withayapayanon, J.H. Harwell, D.A. Sabatini, *J. Surfactants Deterg.* 12 (2009) 91.
- [6] Y. Zhu, V. Molinier, M. Durand, A. Lavergne, J.-M. Aubry, *Langmuir* 25 (2009) 13419.
- [7] M. Durand, Y. Zhu, V. Molinier, T. Feron, J.-M. Aubry, *J. Surfactants Deterg.* 12 (2009) 371.
- [8] Y. Zhu, M. Durand, V. Molinier, J.-M. Aubry, *Green Chem.* 10 (2008) 532.
- [9] D. Abenhaiem, A. Loupy, L. Munnier, R. Tamion, F. Marsais, G. Queguiner, *Carbohydr. Res.* 261 (1994) 255.
- [10] T. Gibson, *J. Org. Chem.* 45 (1980) 1095.
- [11] J.C. Lang, R.D. Morgan, *J. Chem. Phys.* 73 (1980) 5849.
- [12] M.A. Thompson, ArgusLab 4.0.1. Planaria Software LLC, Seattle, WA.
- [13] R. Ahlrichs, M. Baer, M. Haeser, H. Horn, C. Koelmel, *Chem. Phys. Lett.* 162 (1989) 165.
- [14] A. Klamt, G. Schueuermann, *J. Chem. Soc., Perkin Trans. 2* (1993) 799.
- [15] E. Iglesias, J. Anderez, A. Forgiarini, J.-L. Salager, *Colloids Surf., A* 98 (1995) 167.
- [16] O. Mengual, G. Meunier, I. Cayre, K. Puech, P. Snaabre, *Colloids Surf., A* 152 (1999) 111.
- [17] H.G. Bazin, T. Polat, R.J. Linhardt, *Carbohydr. Res.* 309 (1998) 189.
- [18] T. Polat, M. Mohammadi, R.J. Linhardt, *Tetrahedron Lett.* 43 (2002) 8047.
- [19] T. Hikota, M. Nakamura, S. Machida, K. Meguro, *J. Am. Oil Chem. Soc.* 48 (1971) 784.
- [20] C. Vautier-Giongo, B.L. Bales, *J. Phys. Chem. B* 107 (2003) 5398.
- [21] M. Dahanayake, A.W. Cohen, M.J. Rosen, *J. Phys. Chem.* 90 (1986) 2413.
- [22] F. Caboi, A. Chittofrati, P. Lazzari, M. Monduzzi, *Colloids Surf., A* 160 (1999) 47.
- [23] J. Wurtz, J. Meyer, H. Hoffmann, *Phys. Chem. Chem. Phys.* 3 (2001) 3132.
- [24] N. Kallay, V. Tomisic, V. Hrust, R. Pieri, A. Chittofrati, *Colloids Surf., A* 222 (2003) 95.
- [25] B.L. Bales, *J. Phys. Chem. B* 105 (2001) 6798.
- [26] S. Bhattacharya, J. Haldar, *Langmuir* 20 (2004) 7940.
- [27] E. Carey, C. Stubenrauch, *J. Colloid Interface Sci.* 333 (2009) 619.
- [28] S. Pandey, R.P. Bagwe, D.O. Shah, *J. Colloid Interface Sci.* 267 (2003) 160.